The Impact of Protein Corona Morphology on Nanoparticle Diffusion in Biological Fluids: Insights from a Mesoscale Approach - Supporting Material

Beatrice Cipriani[1,2*], Hender Lopez[1*]

[1]School of Physics, Clinical and Optometric Sciences, Technological University Dublin, Grangegorman D07 ADY7, Ireland
[2]FOCAS Research Institute, TU Dublin, City Campus, Dublin 8, Ireland

1 Plasma and corona proteins' details

Table S1: List of proteins characterizing the corona in the P1 NP, with experimental relative abundance obtained from [1] and size derived from the full atomistic structures.

Protein	Relative abundance [%]	Stokes radius [nm]
Kininogen	27.6	5.5
Apolipoprotein E	12.4	2.6
Vitronectin	12.3	4.3
Plasma serine protease inhibitor	5.4	4.9
Fibrinogen	8.4	8.7
Coagulation factor V	4.2	4.8
Isoform 2 of plasma protease C1 inhibitor	3.8	4.5
Plasma kallikrein	3.7	3.4
Coagulation factor XI	2.6	3.5
Histidine-rich glycoprotein	2.4	4.7
Immunoglobulin G	1.8	5.5
Complement C3	1.6	5.2

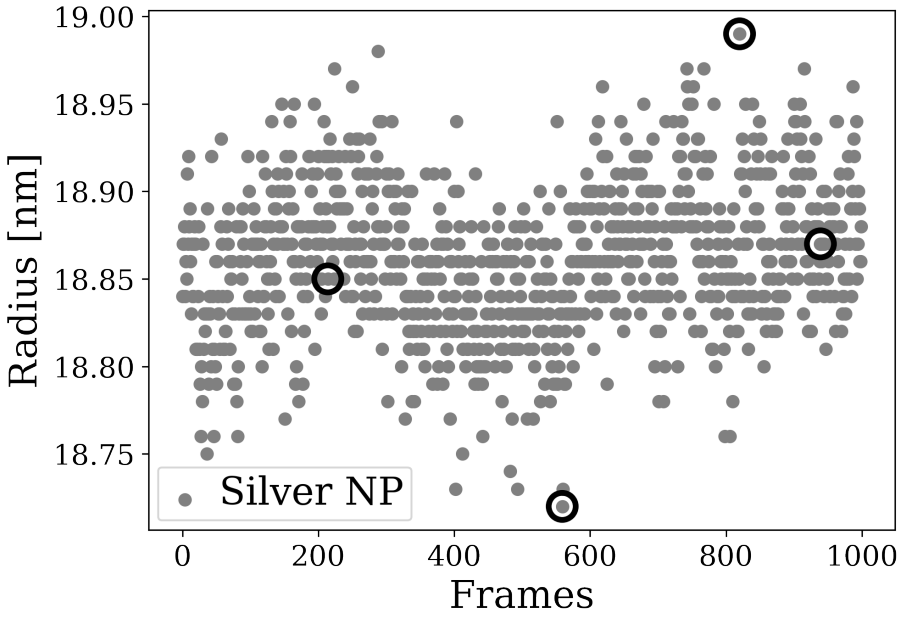

Figure S1: Hydrodynamic sizes of 1000 different morphologies of the PC in the P1 NP. The black circles indicate the morphologies selected in this study. The experimental molarity of each protein is obtained from Ref.[2]

Table S2: List of proteins characterizing the corona in the P2 NP, with experimental relative abundance obtained from [1] and size derived from the full atomistic structures.

Protein	Relative Abundance [%]	Stokes radius [nm]
Fibrinogen	41.1	8.7
ITIH4 protein	16.1	5.4
Kininogen	7.6	5.5
Complement C3	6.3	5.2
Plasma serine protease inhibitor	3.7	4.9
Isoform E of proteoglycan 4	3.0	7.4
Vitronectin	3.0	4.3
Coagulation factor V	1.6	4.8
Apolipoprotein E	1.6	2.6
Coagulation factor XI	1.0	3.5
Carboxypeptidase	1.0	2.8

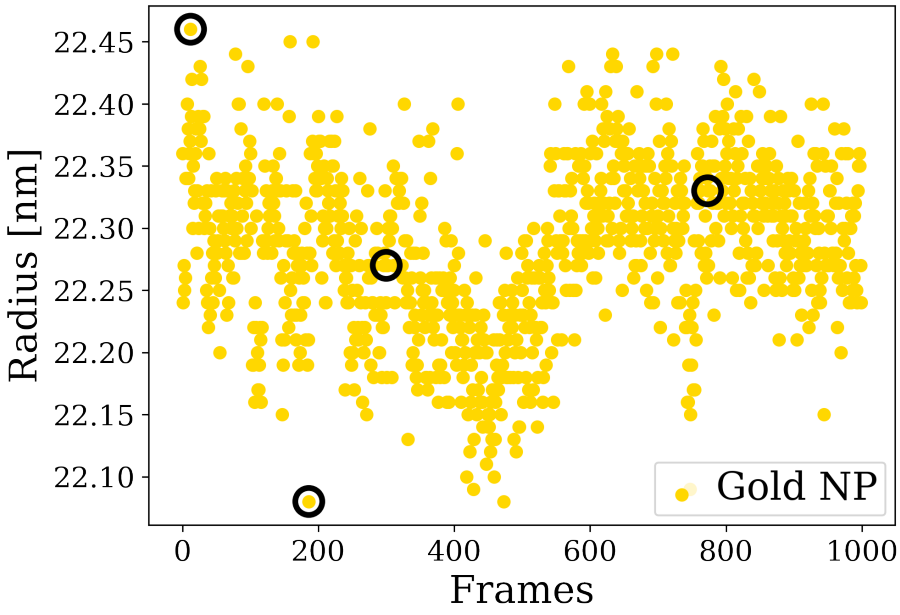

Figure S2: Hydrodynamic sizes of 1000 different morphologies of the PC in the P2 NP. The black circles indicate the morphologies selected in this study.

Name	Structure ID	Molarity [M]	MW [kDa]	r_H [nm]	D_{t_0} [nm^2/μs]	D_{r_0} [μs^{-1}]
Albumin	1AO6	650	66.6	3.5	61.3	3.6
Immunoglobulin G	1HZH	70	151.6	5.5	39.1	0.9
Apolipoprotein A-I	1AV1	54	93.8	4.9	44.1	1.2
Apolipoprotein A-II	P08519	41	11.2	2.4	89.8	9.4
Transferrin	1D3K	35	36.5	2.6	81.4	8.5
α1-Proteinase inhibitor	1ATU	29	42.0	2.9	74.7	6.6
Transthyretin	4TLT	23	13.7	2.4	89.2	11.2
α1-Acid glycoprotein	3APU	21	45.8	2.3	93.1	14.0
Hemopexin	P02790	15	51.7	3.9	55.3	2.5
Immunoglobulin A	1IGA	14	148.6	6.2	34.9	0.8
Apolipoprotein C-III	2JQ3	13	8.8	2.3	92.4	10.7
α2-Macroglobulin	7VON	12	160.1	5.0	42.7	1.2
α2-HS glycoprotein	P02765	12	39.3	3.9	55.5	2.3
Hepatoglobin	P00738	12	45.2	3.7	57.5	2.7
Gc globulin	1J78	11	51.9	3.3	65.7	4.4
Apolipoprotein C-I	P02654	9	9.3	2.1	102.4	15.8
Fibrinogen	3GHG-BA1	9	325.7	8.7	24.6	0.5
Complement C3	2A73	8	185.7	5.2	41.0	1.1
α1-Antichymotrypsin	1AS4	7	42.9	2.8	75.8	7.4
β2-Glycoprotein I	6V06	6	42.6	4.4	49.1	2.1
Vitronectin	P04004	6	54.3	4.3	50.2	1.9
α1-B Glycoprotein	P04217	5	54.3	3.8	56.7	2.7
Apolipoprotein A-IV	3S84	5	63.3	4.0	53.1	2.9
Apolipoprotein C-II	P02655	5	11.3	2.3	93.4	12.23
Ceruloplasmin	4ENZ	3	123.4	4.0	54.3	2.6
Antithrombin III	2B4X	3	99.3	4.0	53.1	2.4
Inter α-trypsin inhibitor	6FPZ	3	74.3	3.5	62.1	3.8
Plasminogen	4DUU	3	88.5	3.8	56.8	2.9
Retinol-binding protein	1RBP	2	21.3	2.2	95.7	14.3

Table S3: Plasma Proteins Data. The 4-character alphanumeric identifiers indicate structures obtained from the Protein Data Bank, while the structures obtained from Alphafold are indicated with the letter P followed by five numbers. r_H indicates the hydrodynamic radius, D_{t_0} and D_{r_0} are the translational and rotational diffusion coefficients, respectively, derived from the crystal structure in pure solvent with HYDROPRO [3]

2 Mean Squared Displacement

In the work, Brownian Dynamics was employed and its validity to be used for the systems studied was determined by comparing the relevant time scales present in the simulation with the momentum relaxation time of the different components of the system. The momentum relaxation time is given by $\tau = \frac{m}{\gamma}$, where m is the mass of the simulated bead and γ is its friction coefficient. For spherical particles, $\gamma = 6\pi\eta R$, where η is the viscosity of the medium (in our case 10^{-3} Pa·s, assuming water at room temperature) and R is the radius of the particle (more precisely the hydrodynamic radius used to model the diffusivity of the beads). In our simulations, the largest sphere corresponds to NP-PC complexes of ∼25 nm in radius, while the smallest sphere is for the protein ApoC1 (2.10 nm in radius). For the NP-protein complexes, assuming a mass of 5.3×10^4 kDa (estimated using a 10 nm in radius NP with a bulk density of gold of 19.3 g/cm^{-3} and 4000 kDa for the protein corona of the P2 system) we obtain a $\tau \sim 2 \times 10^{-10}$ s. For ApoC1, using a mass of 9.33 kDa and a hydrodynamic radius of 2.10 nm, the corresponding relaxation time is $\tau \sim 4 \times 10^{-13}$ s. Typical diffusion timescales for nanoparticle or protein displacements over nanometer distances are in the microsecond to millisecond range, yielding a separation of at least 6–9 orders of magnitude relative to τ. This firmly places all components of the system in the overdamped regime and justifies the use of Brownian dynamics.

We verified that all simulated particles reach the long-time diffusive regime. The log-log plots of the MSD vs. time were analysed and the linear fits of the MSD vs. time curves were performed for the long (i.e. "diffusive") regimes. After a short anomalous intermediate regime, the MSD recovers a linear scaling with time. The particles are considered in the diffusive regime when the slope from a log-log plot of the MSD is approximately 1 [4]. From the linear fit with the MSD in long-time, normal, diffusive regime, the translational diffusion coefficient is obtained as

$$D_t = \frac{m}{6} \tag{S1}$$

with m slope of the linear fit.

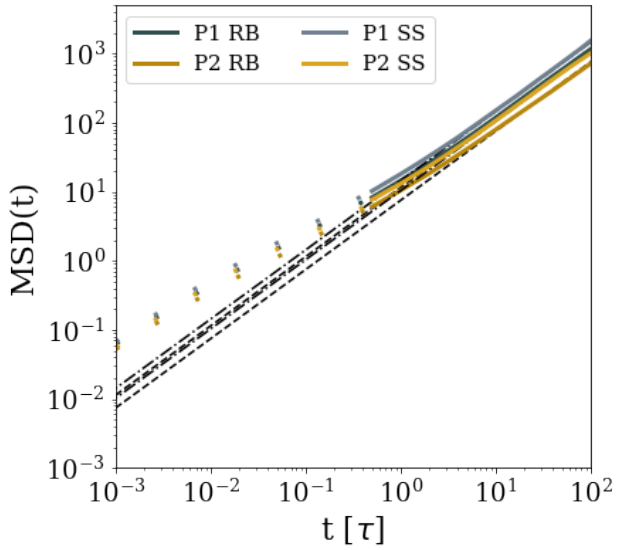

Figure S3: Ensemble-averaged, center-of-mass MSD(t) for P1 and P2 systems in polydisperse, plasma medium at ϕ=0.3. Black dashdot/dashed lines correspond to fits to the long-time regime

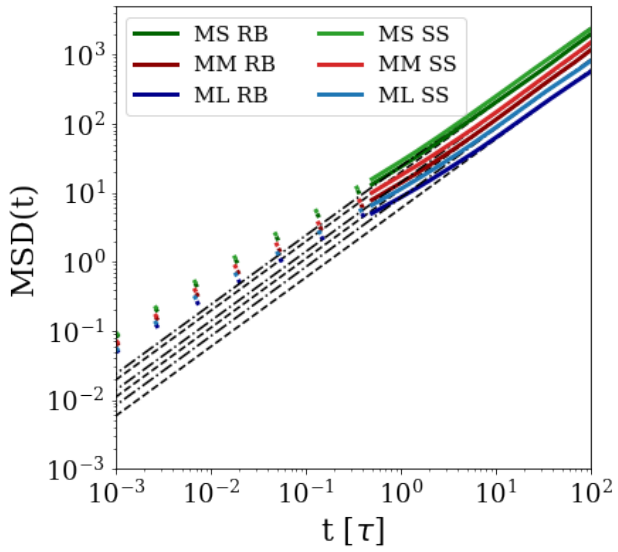

Figure S4: Ensemble-averaged, center-of-mass MSD(t) for MS, MM and ML systems in polydisperse, plasma medium at ϕ=0.3. Black dashdot/dashed lines correspond to fits to the long-time regime

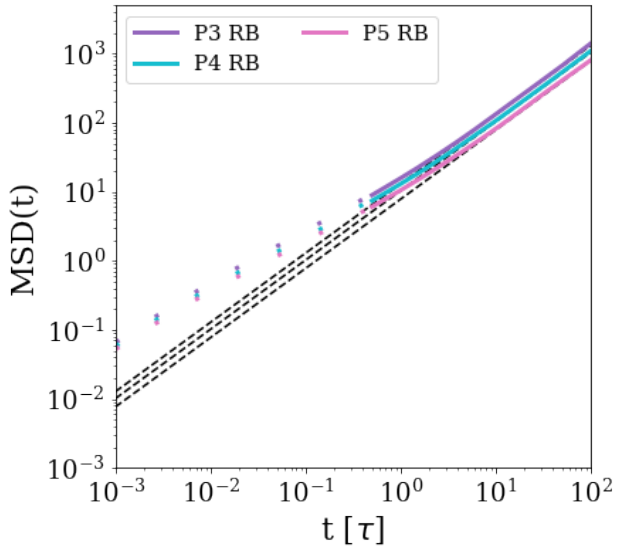

Figure S5: Ensemble-averaged, center-of-mass MSD(t) for P3, P4 and P5 systems in polydisperse, plasma medium at ϕ=0.3. Black dashdot/dashed lines correspond to fits to the long-time regime

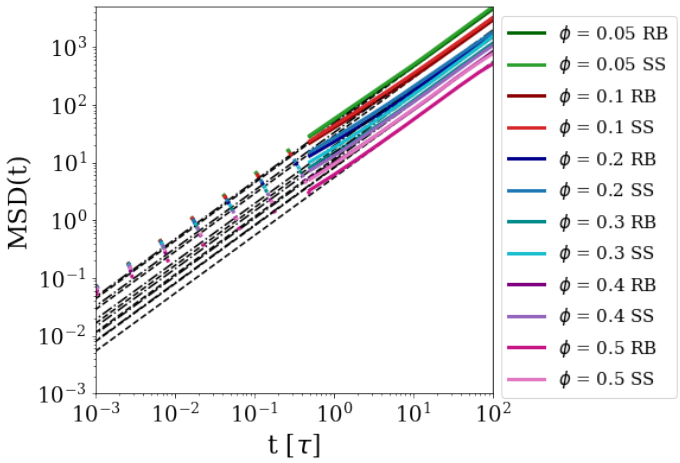

Figure S6: Ensemble-averaged, center-of-mass MSD(t) for P1 systems in Medium #0 (polydisperse plasma). Black dashdot/dashed lines correspond to fits to the long-time regime

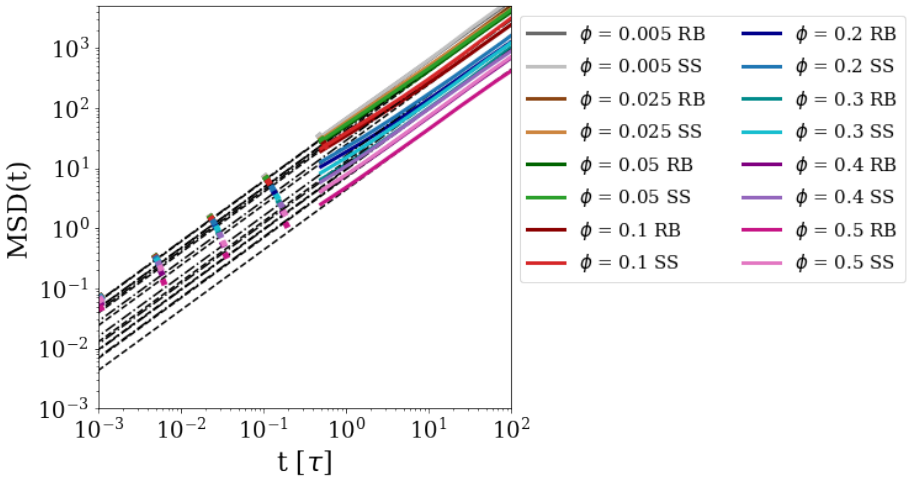

Figure S7: Ensemble-averaged, center-of-mass MSD(t) for P1 systems in Medium #1 (one type of crowder). Black dashdot/dashed lines correspond to fits to the long-time regime

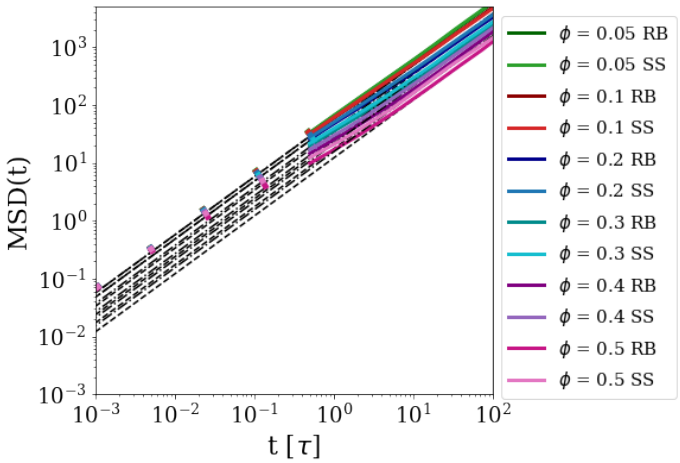

Figure S8: Ensemble-averaged, center-of-mass MSD(t) for P1 systems in Medium #5 (one type of crowder). Black dashdot/dashed lines correspond to fits to the long-time regime

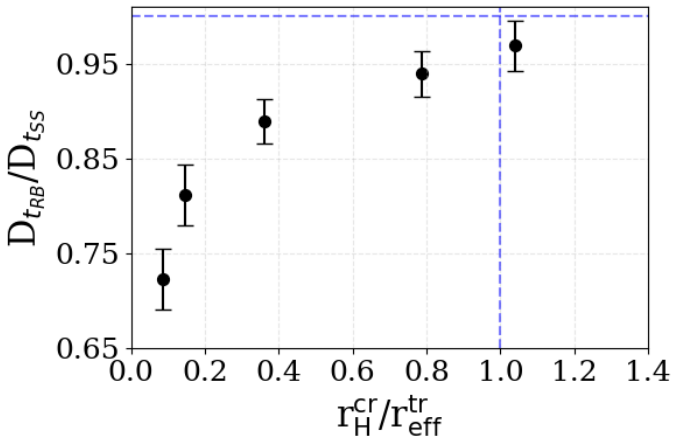

Figure S9: RB diffusivities normalised over the equivalent h-SS ones plotted as a function of the size ratio between crowders and tracer's hydrodynamic radius $r_{\mathrm{eff}}^{\mathrm{tr}}$. Blue dashed lines indicate the ideal case where the RB and h-SS diffusivities coincide ($D_{\mathrm{t_{RB}}}/D_{\mathrm{t_{SS}}} = 1$) for a size ratio of 1.

References

[1] W. Lai, Q. Wang, L. Li, Z. Hu, J. Chen, and Q. Fang, "Colloids and Surfaces B : Biointerfaces Interaction of gold and silver nanoparticles with human plasma : Analysis of protein corona reveals specific binding patterns," *Colloids and Surfaces B: Biointerfaces*, vol. 152, pp. 317–325, 2017.

[2] G. L. Hortin, "The MALDI-TOF mass spectrometric view of the plasma proteome and peptidome," *Clinical Chemistry*, vol. 52, no. 7, pp. 1223–1237, 2006.

[3] A. Ortega, D. Amorós, and J. García De La Torre, "Prediction of hydrodynamic and other solution properties of rigid proteins from atomic- and residue-level models," *Biophysical Journal*, vol. 101, no. 4, pp. 892–898, 2011.

[4] E. J. Maginn, R. A. Messerly, D. J. Carlson, D. R. Roe, and J. R. Elliot, "Best Practices for Computing Transport Properties 1. Self-Diffusivity and Viscosity from Equilibrium Molecular Dynamics [Article v1.0]," *Living Journal of Computational Molecular Science*, vol. 2, no. 1, pp. 1–20, 2020.